ПО ИТОГАМ ПРОЕКТОВ
РОССИЙСКОГО ФОНДА ФУНДАМЕНТАЛЬНЫХ ИССЛЕДОВАНИЙ
Проект РФФИ # 12-02-00421-а

Microscopic theory of vortex pinning on columnar defects in conventional and chiral superconductors

A. S. Mel'nikov[+*1)], *A. V. Samokhvalov*[+*], *V. L. Vadimov*[+]

[+]*Institute for Physics of Microstructures of the RAS, 603950 Nizhny Novgorod, Russia*

[*]*Lobachevsky State University of Nizhny Novgorod, 603950 Nizhny Novgorod, Russia*

Submitted 10 October 2015

The mechanisms of individual vortex pinning and stability of multivortex configurations in different superconducting compounds and artificial structures are analyzed on the basis of microscopic theory which allowed to describe the corresponding modification of the anomalous spectral branches in the quasiparticle spectrum caused by the electron scattering at the defect. The individual pinning potentials and corresponding depinning currents are evaluated. The experimentally observable consequences for the scanning tunneling microscopy characteristics and high-frequency field response are discussed. The comparative study of the conventional and chiral superconductors allowed to suggest experimental tests probing the superconducting gap symmetry. The chiral superconductors are shown to reveal a strong dependence of the pinning characteristics on the mutual orientation of the magnetic field and internal angular momentum of the Cooper pair.

DOI: 10.7868/S0370274X15230150

The physics of interaction between vortices and defects is known to form the basis for understanding of the key experimental phenomena in the critical and resistive states in type-II superconductors. This is why this subject has continued to attract the interest of researchers for several decades. One of the fundamental contribution to this field has been made in 1971 by Mkrtchyan and Shmidt who suggested a phenomenological theory of vortex pinning at cylindrical insulating inclusions [1]. Further this model has been developed in Refs. [2–4], in particular, in the context of experimental works on the effect of columnar defects created, e.g., by the ion irradiation on the critical currents. Despite of the obvious success of the Mkrtchyan–Shmidt model this London-type theory possesses obvious shortcomings if applied for description of rather small defects of the size comparable with the superconducting coherence length ξ and especially for the limit of low temperatures far from the critical temperature T_c. The nonlocal nature of superconducting correlations in this case is responsible for the additional contribution to the gain in the condensation energy for the pinned vortex which breaks down the simple proportionality of this gain to the defect volume [5–7]. The deeper understanding of the pinning phenomena becomes even more important if we turn to the physics of vortex matter in superconductors with the unconventional pairing. The physics of defects in these systems can not be reduced only to the Mkrtchyan–Shmidt mechanism, i.e., to the interaction of the real and image vortices or the change in the condensation core energy due to a nontrivial structure of the superconducting state around the bare defects even without trapped vortices. The London-type theory also appears to be insufficient for an adequate description of dynamics of pinned vortices under the influence of the ac transport current. Such description is particularly important for the analysis of the effect of vortices on the microwave response. Indeed, the ac transport currents exciting the pinned vortex oscillations cause the drag of both Cooper pairs and the unpaired quasiparticles inside the moving vortex cores. It is the consideration of combined dynamics which is necessary for the correct calculations of the dissipative and Hall parts of the vortex response [8].

[1)]e-mail: melnikov@ipm.sci-nnov.ru

In order to reveal the microscopic pinning mechanisms we choose to study a model problem of a single vortex trapped by the columnar defect within the quasiclassical version of the Bogolubov–de Gennes theory. The defect is assumed to be an insulating cylinder of the radius R well exceeding the Fermi wavelength $\lambda_F = 2\pi/k_F$. Within the quasiclassical approach such defects cause just a reflection of the straight quasiparticle trajectories from the defect surface as it is shown in Fig. 1. In the absence of this trajectory scattering, i.e., for a free vortex this model should give us a standard Caroli–de Gennes–Matricon (CdGM) quasiparticle spectral branch [9]. This subgap branch called also an anomalous one changes from $-\Delta_0$ to $+\Delta_0$ with the change in the angular momentum μ. At small energies $|\varepsilon| \ll \Delta_0$ we get $\varepsilon \simeq \mu\omega_0$, where $\omega_0 \simeq \Delta_0/k_F\xi$ for a two-dimensional case. The angular momentum should be defined from the Bohr–Sommerfeld quantization rule. The resulting μ values appear to depend on the gap structure in the momentum space: for s-wave (p-wave) pairing μ is half an odd integer (an integer). In three dimensions the energy spacing ω_0 becomes a function of the quasiparticle momentum projection at the vortex axis.

This textbook picture is strongly modified by the presence of the trajectory scattering since the subgap spectrum is extremely sensitive to the superconducting phase difference at the ends of the quasiparticle trajectory crossing the vortex core. It is instructive to mention here the analogy with the quasiparticle spectrum in Josephson junctions where the subgap levels $\varepsilon = \pm\Delta_0 \cos(\varphi/2)$ are also determined by the phase difference φ at the ends of the trajectory passing between two superconducting electrodes [10]. For a free vortex this phase difference equals to π which gives us zero energy level. Further application of the perturbation theory in the superfluid velocity allows to get the dependence of the CdGM branch on μ. Considering pinned vortices one can easily make an important observation: the quasiparticle reflection at the defect surface causes strong deviations of the phase φ from π. These deviations appear for trajectories with the impact parameters $b = -\mu/k_F$ less than the defect radius R (trajectory *2* in Fig. 1) otherwise the trajectory does not touch the defect surface (trajectory *1* in Fig. 1). Such scattering obviously causes a repulsion of the energy levels from zero (Fermi level) destroying, thus, the CdGM spectrum. It is quite natural to assume that the effective minigap in the spectrum of a pinned vortex should scale linearly with the defect radius; $\Delta_m \simeq \omega_0 k_F R$. The vortex escape from the defect should be accompanied by the corresponding transformation of the subgap spectrum, i.e., by closing of this minigap. The phase φ is affected not only by the vortex winding number in the coordinate space. The winding number in the momentum space which appear, e.g., in the p-wave case can also change this phase difference for trajectories experiencing normal scattering at the defect. As a result, the defects in p-wave superconductors can produce anomalous spectral branches even in the absence of vortices. Being somewhat similar to the anomalous vortex branches these quasiparticle states carry circulating currents which cause a vortex-defect interaction strongly dependent on the mutual orientation of vorticities in coordinate and momentum spaces.

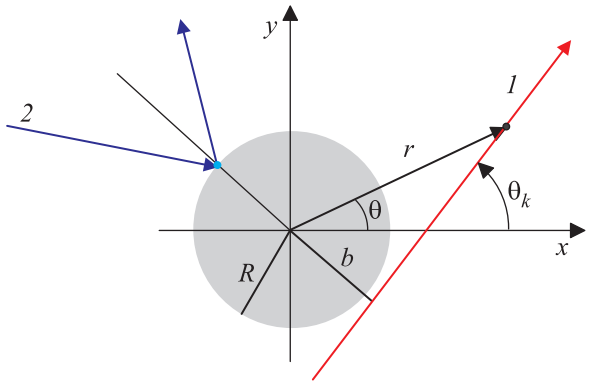

Fig. 1. (Color online) Quasiclassical trajectories passing through the core of a vortex pinned by an insulating defect

The remaining part of the paper is organized as follows. First, we introduce the basic quasiclassical equations used in our calculations. Then we briefly review the results obtained for the quasiparticle spectra for pinned vortices in s- and p-wave compounds accompanying this consideration by the analysis of the corresponding pinning potential. Second, we consider some dynamic effects arising from the modification of the anomalous spectral branches and analyze possible experimental predictions for a microwave response in the vortex state.

1. Basic quasiclassical equations. We consider a columnar defect as an insulator cylinder of the radius R. The magnetic field $\mathbf{B}$ is parallel to the cylinder axis z, the vortex axis coincides with the cylinder axis. Thus, the system is invariant with respect to the translations along the z-axis and the rotations around it. For simplicity we restrict ourselves with a two-dimensional case and consider a motion of quasiparticles only in the (x, y) plane. The excitation spectrum can be obtained from the quasiclassical version of the Bogolubov–de-Gennes equations written for a two-component quasiparticle wave function $\psi(\mathbf{r}) = (u,\ v)$:

$$-i\hbar v_F \hat{\tau}_3 \frac{\partial \psi}{\partial s} + [\hat{\tau}_+ \Delta(\mathbf{r}, \theta_k, b) + \text{h.c.}]\, \psi = \epsilon\psi, \qquad (1)$$

where $\hat{\tau}_\pm = (\hat{\tau}_1 \pm i\hat{\tau}_2)/2$, $\hat{\tau}_1$, $\hat{\tau}_2$, and $\hat{\tau}_3$ are the Pauli matrices in the Nambu space, $\hbar k_\mathrm{F}$ is the Fermi momentum, $mv_\mathrm{F} = \hbar k_\mathrm{F}$, Δ is the quasiclassical form of the gap operator, $b = -\mu/k_\mathrm{F}$ is the trajectory impact parameter, and s is a coordinate along the classical trajectory (see Fig. 1). The angle θ_k defines the trajectory direction in the (x, y) plane. The transition from the (s, b) coordinates to the usual cartesian (x, y) coordinates can be performed as follows:

$$x = s\cos\theta_k - b\sin\theta_k,\ y = s\sin\theta_k + b\cos\theta_k. \qquad (2)$$

Considering an extreme type-II superconductor with a large London penetration depth $\lambda \gg \xi$ we neglect the vector potential of the magnetic field $A_\theta \approx Br/2$ because its contribution to the superfluid velocity $A/\Phi_0 \propto \propto r/\lambda^2$ is small compared to the gradient of the order parameter phase $\propto 1/r$. Here r and θ are the polar coordinates and Φ_0 is the magnetic flux quantum. The full wavefunction can be expressed through its quasiclassical counterpart:

$$\Psi(r,\theta) = \int_0^{2\pi} e^{ik_\mathrm{F} r\cos(\theta_k-\theta)} e^{iS(\theta_k)} \psi[r\cos(\theta_k-\theta),\theta_k]\frac{d\theta_k}{2\pi}. \qquad (3)$$

Here $S(\theta_k)$ is the angular eikonal connected to the angular momentum via the expression $\mu = \partial S/\partial\theta_k$. The angular momentum μ is conserved due to the axial symmetry of the system. We assume that the quasiparticle wavefunction does not penetrate the defect and impose the zero boundary conditions at the defect surface:

$$\int_0^{2\pi} e^{ik_\mathrm{F} R\cos\theta_k + i\mu\theta_k}\psi\left(R\cos\theta_k\right) d\theta_k = 0. \qquad (4)$$

Supposing the argument of the exponent to vary rather fast we can use the stationary phase method in order to evaluate the integral. The stationary phase points are given by the equation $\sin\alpha = \mu/k_\mathrm{F}R = -b/R$. This equation has no solutions if the impact parameter is greater than the defect radius and as a result the defect does not affect the wave function at such trajectories. In the opposite case $|b| < R$ there are two stationary angles $\theta_1 = -\arcsin(b/R)$ and $\theta_2 = \pi - \theta_1$ which correspond to the incident and reflected classical trajectories. The sum of the two contributions provides the boundary condition for the quasiclassical wavefunction.

2. Pinned vortices in *s*-wave superconductors. We start with the analysis of the subgap spectrum for a vortex trapped by the columnar defect in superconductors with s-wave pairing. The order parameter $\Delta(r,\theta)$ takes the form

$$\Delta = \Delta_0 f^{(m)}(r)e^{im\theta}, \quad r = \sqrt{x^2+y^2} \geq R, \qquad (5)$$

where Δ_0 is a gap value far from the vortex core, m is the vorticity in the real space, and $f^{(m)}(r)$ is the coordinate depending order parameter for a vortex centered at $r = 0$, such that $f^{(m)}(r)$ saturates at unity at large $r \gg \xi$. In $(s,\ \theta_k)$ variables one obtains the following order parameter profile at the classical trajectory for $r = \sqrt{s^2+b^2} \geq R$:

$$\Delta/\Delta_0 = D_b^{(m)}(s)e^{im\theta_k}, \qquad (6)$$

$$D_b^{(m)}(s) = f^{(m)}(\sqrt{s^2+b^2})\left(\frac{s+ib}{\sqrt{s^2+b^2}}\right)^m. \qquad (7)$$

The cylindrical symmetry of our system allows to separate the θ_k-dependence of the function

$$\psi(s,\theta_k) = e^{i(m\hat{\tau}_3/2)\theta_k}\widetilde{\psi}(s) \qquad (8)$$

and the Eq. (1) reads:

$$-i\xi\hat{\tau}_3\frac{\partial\widetilde{\psi}}{\partial s} + \Delta_b^{(m)}\widetilde{\psi} = \varepsilon\widetilde{\psi}, \qquad (9)$$

where $\xi = \hbar v_\mathrm{F}/\Delta_0$ is the coherence length, $\varepsilon = \epsilon/\Delta_0$ and the gap operator takes form

$$\Delta_b^{(m)} = \hat{\tau}_1\,\mathrm{Re}D_b^{(m)} - \hat{\tau}_2\,\mathrm{Im}D_b^{(m)}. \qquad (10)$$

The symmetry properties of both the gap operator $\hat{\Delta}_b(s)$ and the solution of Eq. (9) depend on the vorticity m:

$$\Delta_b^{(m)}(-s) = \begin{cases} \Delta_b^{(m)*}(s), & \text{for even } m, \\ -\Delta_b^{(m)*}(s), & \text{for odd } m, \end{cases} \qquad (11)$$

$$\widetilde{\psi}(-s) = \begin{cases} C\tau_1\widetilde{\psi}(s), & \text{for even } m, \\ C\tau_2\widetilde{\psi}(s), & \text{for odd } m, \end{cases} \qquad (12)$$

where C is a constant dependent on the boundary condition at the surface of the insulating cylinder. Using the stationary phase method we can write this boundary condition (4) for the wave functions $\widetilde{\psi}(s)$ in the form:

$$e^{i\varphi_0}\widetilde{\psi}(s_0) = e^{-i\varphi_0}\widetilde{\psi}(-s_0), \qquad (13)$$

where $s_0 = \sqrt{R^2-b^2}$ and

$$\varphi_0 = k_\mathrm{F}s_0 + (\mu + m\hat{\tau}_3/2)(\theta_1-\theta_2)/2 + \pi/4. \qquad (14)$$

For $|\,b\,| > R$ we can put $s_0 = 0$ and $\theta_1 - \theta_2 = -\pi$ in the expression (14).

A singly quantized vortex. The subgap spectrum of a singly quantized vortex ($m = 1$) trapped by the columnar defect of the radius R has been analyzed within the quasiclassical approach in Ref. [11]. To develop an analytical description we applied the standard method

[12] based on the perturbation theory in Eq. (9) with respect to the imaginary part of the gap function (10). For rather large impact parameters $|b| > R$ ($|\mu| > \mu_R = k_F R$) quasiclassical trajectories of electron–hole excitations do not experience reflection at the defect surface and, thus, the subgap spectrum coincides with the CdGM one

$$\varepsilon_0(b) = \frac{b}{I_0}\int\limits_{-\infty}^{+\infty} ds \frac{f^{(1)}(\sqrt{s^2+b^2})}{\sqrt{s^2+b^2}} e^{-2K_0(s)/\xi}, \qquad (15)$$

$$K_0(s) = \int\limits_0^s dt \mathrm{Re}\,\widetilde{D}_b^{(1)}(t), \; I_0 = \int\limits_{-\infty}^{+\infty} ds e^{-2K_0(s)/\xi}.$$

In the opposite case $|b| \le R$ ($|\mu| \le \mu_R$) the normal reflection of trajectories at the defect destroys the low energy part of CdGM spectral branch: with the decrease in $|b|$ below the threshold value R the energy of the subgap bound state rapidly approaches the superconducting gap Δ_0

$$\varepsilon_s(b) = \frac{\chi}{I}\int\limits_{-\infty}^{+\infty} ds \, \frac{f^{(1)}[\sqrt{(|s|+s_0)^2+b^2}]}{\sqrt{(|s|+s_0)^2+b^2}} \times \qquad (16)$$

$$\times \left(R + |s|\sqrt{1-b^2/R^2}\right) e^{-2K(s)/\xi}, \; \chi = \mathrm{sign} b,$$

$$K(s) = \chi \int\limits_0^s dt \, \mathrm{Re}\, G(t), \quad I = \int\limits_{-\infty}^{+\infty} ds \, e^{-2K(s)/\xi},$$

$$G(s) = -\frac{f^{(1)}[\sqrt{(|s|+s_0)^2+b^2}]}{\sqrt{(|s|+s_0)^2+b^2}} \times \qquad (17)$$

$$\times \left[sb/R + i\left(R + |s|\sqrt{1-b^2/R^2}\right)\right].$$

It is evident that $\varepsilon_s(R) = \varepsilon_0(R)$ and, thus, the expressions (15) and (16), (17) describe the spectrum $\varepsilon(b)$ for an arbitrary impact parameter b:

$$\varepsilon(b) = \begin{cases} \varepsilon_s(b), & |b| \le R, \\ \varepsilon_0(b), & |b| > R. \end{cases} \qquad (18)$$

Fig. 2 shows a typical plot of the quasiparticle spectrum obtained analytically, i.e., using Eq. (18), and numerically. We choose a simple model dependence

$$f^{(1)}(r) = r/\sqrt{r^2+\xi^2}, \qquad (19)$$

neglecting, thus, the influence of the defect on the behavior of the gap profile. Due to the spectrum symmetry properties $\varepsilon(-b) = -\varepsilon(b)$ we plot in Fig. 2 only the spectrum for positive energies $\varepsilon > 0$. To find the spectral

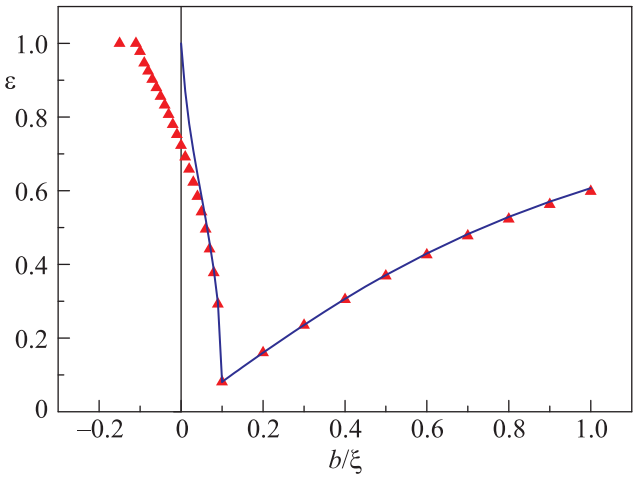

Fig. 2. (Color online) The quasiparticle spectrum as a function of the impact parameter b, obtained from the numerical solution of the eigenvalue problem (9), (13), (14), is shown by red triangles. The spectral branches calculated using Eq. (18) are shown by blue solid lines. Here we put $R = 0.1\,\xi$, $k_F\xi = 200$

branch $\varepsilon(b)$ numerically we solve the eigenvalue problem (9), (13), (14), for $s \ge s_0$ requiring the decay of the wave function $\widetilde{\psi}$ at $s \to \infty$. Thus, contrary to the CdGM case the subgap spectral branch of the pinned vortex does not cross the Fermi level: there appears a minigap $\Delta_m(R) \simeq |\varepsilon_0(R)|$ in the quasiparticle spectrum. The results are in a good agreement with the calculation of the quasiparticle spectrum [13] using the Bogolubov–de Gennes equations within the range of applicability of the quasiclassical approximation $k_F\xi \gg 1$. The minigap Δ_m grows with the increase in the cylinder radius R.

The minigap in the spectrum of quasiparticles should result in peculiarities of the local density of states (LDOS) and can be probed by the STM measurements. The typical plot of the local differential conductance

$$\frac{dI/dV}{(dI/dV)_N} = \int\limits_{-\infty}^{\infty} d\varepsilon \, \frac{N(\mathbf{r},\,\varepsilon)}{N_0} \frac{\partial f(\varepsilon - eV)}{\partial V}, \qquad (20)$$

$$N(r,\,\varepsilon) = k_F \int db \, \frac{\exp\left[-2K_b\left(\sqrt{r^2-b^2}\right)\right]}{2\pi k_F I_b \sqrt{r^2-b^2}} \delta[\varepsilon - \varepsilon(b)],$$

vs the bias voltage eV at various distances r from the cylinder axis is shown in Fig. 3. Here we denote

$$K_b(s) = \begin{cases} K(s), & |b| \le R, \\ K_0(s), & R \le |b| \le r, \end{cases}$$

$$I_b = \int\limits_{-\infty}^{+\infty} ds \, e^{-2K_b(s)/\xi}.$$

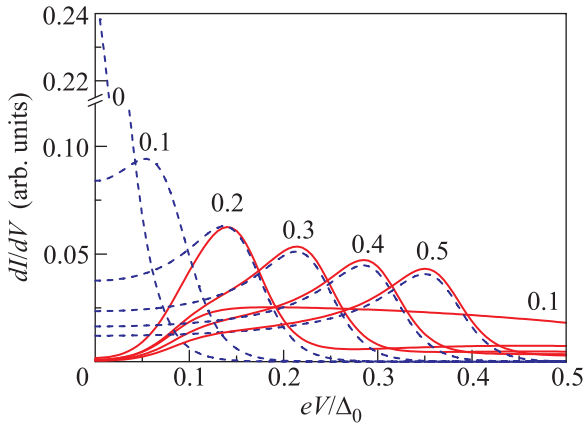

Fig. 3. (Color online) Distribution of the local differential conductance dI/dV as a function of voltage (eV) and distance from the the cylinder axis r. We put here $R/\xi = 0.1$ and $T/\Delta_0 = 0.02$

In accordance with the Landau criterion of superfluidity, the minigap Δ_m, being a hallmark of vortex pinning by an insulating columnar defect, means absence of a flux flow resistivity of a superconductor in the presence of an external current $\mathbf{j}$ driven through the sample. A microscopic scenario of the vortex escape from a columnar defect of a radius $R < \xi$ under the influence of a supercurrent $\mathbf{j} = en_s\mathbf{V}$ applied perpendicular to the vortex axis ($\mathbf{V} = V\mathbf{x}_0$) was proposed in Ref. [14]. The transport supercurrent results in a Doppler shift $\varepsilon_d = (\hbar\mathbf{k}\cdot\mathbf{V})$ of the quasiparticle energy and the subgap spectrum takes the form:

$$\tilde{\varepsilon}(b,\theta_k) = \varepsilon(b) + \hbar k_{\mathrm{F}} V\cos\theta_k. \qquad (22)$$

At the critical current $j_L = en_sV_L$ ($V_L = \Delta_m/\hbar k_{\mathrm{F}}$) the minigap Δ_m in the spectrum (22) disappears and the Doppler-shifted branch of the quasiparticle spectrum crosses the Fermi level. This first topological electronic transitions in the vortex core is associated with the opening of Fermi surface (FS) segments and corresponds to the creation of a vortex-antivortex pair bound to the defect. The corresponding critical current density can be expressed via the CdGM spectrum $\varepsilon_0(b)$ (15): $j_L \simeq j_cR/\xi$ for $R \ll \xi$ and $T \to 0$. Here $j_c = ek_{\mathrm{F}}^2\Delta_0/3\pi^2\hbar$ is the depairing current density. Several scenarios of destruction of the bound vortex configuration were suggested [14]: (i) the FS segments can merge due to quantum mechanical Landau–Zener tunneling; (ii) the spectral flow through the energy gap can occur due to the impurity scattering between different FS segments; (iii) the free vortex can be formed when the Doppler shift reaches the gap value, i.e., the current density j approaches the depairing one j_c. This second transition accompanied by the change in the Fermi surface topology occurs at the critical current j_d ($j_L < j_d \leq j_c$) and corresponds to the formation of a free vortex, i.e., determines the depinning transition at dc currents.

Multiquanta vortices. The above arguments regarding the relation between the stability of a pinned vortex and Landau criterion appear to be useful also for the analysis of stability of a multiquantum vortex state which is intensively studied in the samples with antidots [15, 16]. The multiquanta vortices are known to be trapped at columnar defects either for a rather large defect radius [1, 17, 18] or for the mixed state in mesoscopic samples [19, 20]. In the absence of defects the spectrum of a multiquantum vortex with the vorticity m is known to consist of m anomalous energy branches [12]. The behavior of these branches has been previously investigated both numerically and analytically [12, 21–26]. The spectrum of a multiquantum vortex pinned at a columnar defect was calculated in Ref. [11]. The typical plots of quasiparticle spectra obtained from the numerical solution of the eigenvalue problem (9), with the boundary condition (13), (14) for vortices with winding numbers $m = 2, 3$ are shown in Fig. 4. Similarly to the case of a singly quantized vortex the small b part of the spectrum is formed by the spectral branches induced by the normal scattering at the defect. These branches transform into the standard anomalous ones with the increase in the $|\,b\,|$ value. With the increase in the cylinder radius all the spectral branches appear to be expelled from the Fermi level.

According to a simple phenomenological estimate [1] based on the London-type theory the maximum number M_Φ of flux quanta which can be trapped by the cylindrical cavity of the radius R is determined by the expression: $M_\Phi \sim R/2\xi$. This estimate gives us the critical radii of the defects which can trap the two and three vortices, respectively: $R^{(2)} \simeq 4\xi$ and $R^{(3)} \simeq 6\xi$. To improve this criterion one can apply the above results for the quasiparticle spectra of a pinned multiquantum vortex. Indeed, using the Landau criterion (i.e., the condition of the absence of the quasiparticle states at the Fermi surface) we find that the expressions for the above critical radii of the defects read: $\widetilde{R}^{(2)} \simeq 0.8\xi$ and $\widetilde{R}^{(3)} \simeq 1.4\xi$ for $M_\Phi = 2\,, 3$, respectively (see Fig. 4). Note that microscopic criterion of the M_Φ-quantum vortex trapping predicts much smaller critical radii comparing to the phenomenological ones: $\widetilde{R}^{(M)} \ll R^{(M)}$.

In order to verify the validity of the Landau-type criterion we have carried out the self-consistent numerical analysis of the trapped multivortex state stability taking account of the modification of the gap profile $\Delta(r)$ near the defect and the contribution of delocal-

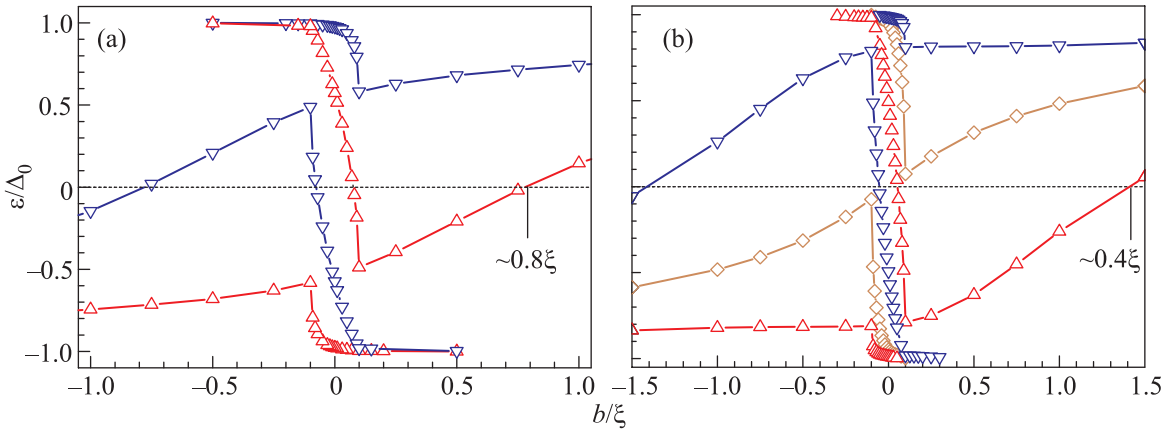

Fig. 4. (Color onkine) The spectral branches as functions of the impact parameter b, obtained from the numerical solution of the eigenvalue problem (9), (13), (14) for $m = 2$ (a) and 3 (b) ($R = 0.1\xi$, $f^m(r) = (f^1)^m$)

ized excitations. Our analysis is based on the solution of the Eilenberger equations for quasiclassical propagators along the trajectories. For numerical treatment of these equations we follow the Ref. [27] and introduce a Ricatti parametrization for the Greens functions f and g via the functions a and b

$$f = \frac{2a}{1+ab}, \quad f^\dagger = \frac{2a}{1+ab}, \quad g = \frac{1-ab}{1+ab}, \tag{23}$$

satisfying the nonlinear Riccati equations

$$\hbar v_{\rm F}\, \partial_s a(s) + [2\omega_n + \Delta^* a(s)]\; a(s) - \Delta = 0, \tag{24}$$

$$\hbar v_{\rm F}\, \partial_s b(s) - [2\omega_n + \Delta b(s)]\; b(s) + \Delta^* = 0, \tag{25}$$

where $\omega_n = \pi T(2n+1)$ are the Matsubara frequencies. The solution of the above equations with the self-consistent procedure for the gap function allowed us to find the critical defect radii needed to obtain a stable solution. The simultaneous calculations of the density of states at the Fermi level provide us a possibility to control the validity of the Landau-type criterion. At the temperature $T = 0.05T_c$ these self-consistent simulations give the values $\widetilde{R}^{(2)} \approx 0.44\xi$ and $\widetilde{R}^{(3)} \approx 0.93\xi$ which appear to be even less than the ones found above from the spectrum analysis done for a model gap function profile. This discrepancy is clearly caused by the well-known Kramer–Persch effect [28], i.e., by the vortex core shrinking at low temperatures. Accounting this gap profile transformation the numerical analysis nicely confirms the Landau-type criterion of the stability of multivortex configuration.

3. Pinned vortices in p-wave superconductors. The spectrum of a vortex trapped by the columnar defect in a p-wave superconductor has been analyzed in Ref. [29]. Quasiclassical equations (1) allow to generalize the above consideration taking account of a possible gap anisotropy. Keeping in mind recent experimental and theoretical activity in the study of chiral superconductors [30] and, in particular, in Sr_2RuO_4 we apply this method for the analysis of the electronic structure of pinned vortices in a superconductor with $p_x \pm ip_y$ pairing. The Cooper pairs in such superconductors possess an internal orbital momentum oriented along the z-axis: $l_z = \pm 1$. The quasiclassical order parameter takes the form

$$\Delta(\mathbf{r}, \theta_k) = \Delta_0 \left[\eta_+(\mathbf{r}) e^{i\theta_k} + \eta_-(\mathbf{r}) e^{-i\theta_k}\right], \tag{26}$$

where Δ_0 is a gap amplitude, $\eta_\pm(\mathbf{r})$ are the coordinate dependent order parameters, which describe the Cooper pairs with the opposite angular momenta. Two degenerate ground states are described by the following order parameters: $\eta_+ = 1$, $\eta_- = 0$ and $\eta_- = 1$, $\eta_+ = 0$. Hereafter we call these states as chiral η_+ and η_- domains, respectively.

The axially symmetric vortex solutions are described by the following order parameters [31]:

$$\eta_\pm(\mathbf{r}) = f_\pm^{(m)}(r) e^{i(m\mp 1)\theta}, \tag{27}$$

where m is the sum of the winding numbers in the coordinate and the momentum spaces. One of the functions $f_\pm$ saturates at unity at large $r \gg \xi$ and another one vanishes far from the core. The magnetic flux carried by the vortex is determined by the winding number of the dominating order parameter component, i.e., it is equal to $m+1$ flux quanta for a vortex trapped in the η_- domain and $m-1$ flux quanta for a vortex in the η_+ domain. Thus, there are two different types of singly quantized vortices which are determined by $m = 2$ and 0 in the case of η_+ domain or $m = -2$ and 0 in the case of η_- domain. Without loss of generality we restrict ourselves to the case of η_+ domains and denote

vortices corresponding to $m = 2$ and 0 as N_+ and N_- vortices, respectively.

Similarly to the case of s-wave superconductor, we can introduce the gap function in the terms of trajectory coordinates:

$$D_b^{(m)}(s) = \sum_{\pm} f_{\pm}^{(m)}\left(\sqrt{s^2+b^2}\right)\left(\frac{s+ib}{\sqrt{s^2+b^2}}\right)^{m\mp 1}. \tag{28}$$

Further solution of Eq. (9) with the boundary condition (13) can be obtained using the perturbative procedure developed in the previous sections. Finally one can find the quasiparticle spectrum:

$$\varepsilon_p = \frac{2\chi}{I_p}\int_{s_0}^{+\infty} \mathrm{Im}\left[D_b^{(m)}(s)e^{i\phi}\right] e^{-2K_p(s)}\, ds, \tag{29}$$

$$K_p(s) = \frac{\chi}{\xi}\int_{s_0}^{s} \mathrm{Re}\left[D_b^{(m)}(t)e^{i\phi}\right]\, dt, \tag{30}$$

$$I_p(s) = 2\int_{s_0}^{+\infty} e^{-2K_p(s)}\, ds, \tag{31}$$

where $\phi = (m/2)[\pi - 2\arcsin(b/R)]$ for $b < R$ and $\phi = 0$ for $b > R$, $\chi = \mathrm{sign}(\cos\phi)$.

To verify the approximate solution we have also solved the quasiclassical equations (6), (9), (28) numerically. The results of numerical calculations shown in Fig. 5 demonstrate a good coincidence with the ones obtained using the perturbation approach except the energies close to the superconducting gap Δ_0. The failure of the perturbation procedure in this limit arises from the divergence of the wave function localization radius. The spectrum of the N_- vortex only slightly differs from the CdGM solution (see Fig. 5). In this state the order parameter vorticity in the **r**-space is compensated by its chirality in **k**-space and the phase difference at the ends of every classical trajectory is always equal to π. The defect effectively changes the order parameter amplitude along the trajectory and slightly modifies the spectrum.

In opposite, for the N_+ vortex the phase difference at the ends of classical trajectory causes a significant spectrum modification even for small impact parameters (see Fig. 5). As a result, the subgap spectrum consists of three branches. Within the perturbation approach these branches reveal themselves in the spectrum discontinuity at the points $b = \pm R/\sqrt{2}$, where perturbation theory is not applicable. There are two branches which transform into the CdGM branch at large $|b| > R$ and approach the superconducting gap at small b. The similar spectral branches have been found in previous sections in the spectrum of a pinned vortex in the s-wave

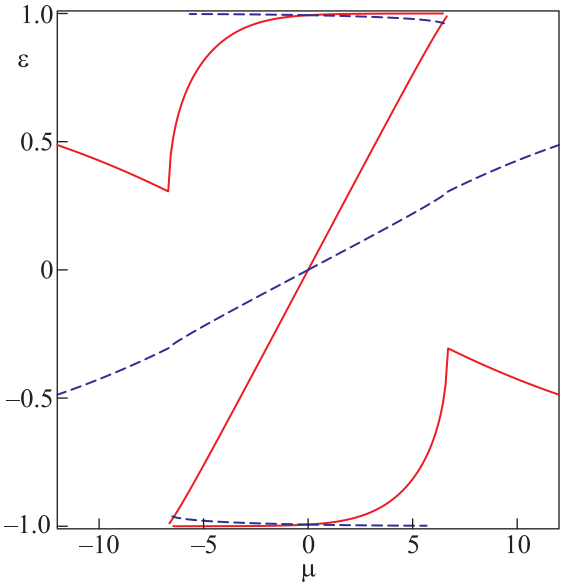

Fig. 5. (Color online) Numerical solution of the quasiclassical Eq. (9) for p-wave superconductor. Solid red line and dashed blue line stand for the spectrum of quasiparticles in N_+ and N_- vortices, respectively. The defect radius is $R = 0.4\xi$

superconductor. In addition to these branches there is an almost linear branch that goes through the origin with the slope inversed with respect to the CdGM solution (cf. the introductory section). We propose that this branch corresponds to the edge states bound to the surface of the unconventional superconductor. The spectrum of these surface states can be easily found within the quasiclassical approach solving the Eq. (9) with $D = \exp(i\theta_k)$ that corresponds to the homogeneous chiral domain. Performing the same calculations as we had done for a vortex, we will obtain the following spectrum:

$$\varepsilon_b = \begin{cases} -\dfrac{b}{R}, & |b| < R, \\ -\mathrm{sign}b, & |b| > R. \end{cases} \tag{32}$$

This quasiparticle spectrum is very close to the anomalous spectral branch in Fig. 5, so we can claim that this branch corresponds to the surface states. The spectrum of quasiparticles in the N_- vortex does not contain the edge states branch and it means that the N_- vortex suppresses the edge states for rather small defects $R \lesssim \xi$. In the opposite limit $R \gg \xi$ we can expect that the spectra of quasiparticles in both vortices are similar to the spectra of the defect, because the superfluid velocity decays as $1/r$ and the major contribution to the quasiparticle energy arises from the internal chirality of the superconductor. Note that recent numerical calculations [32]

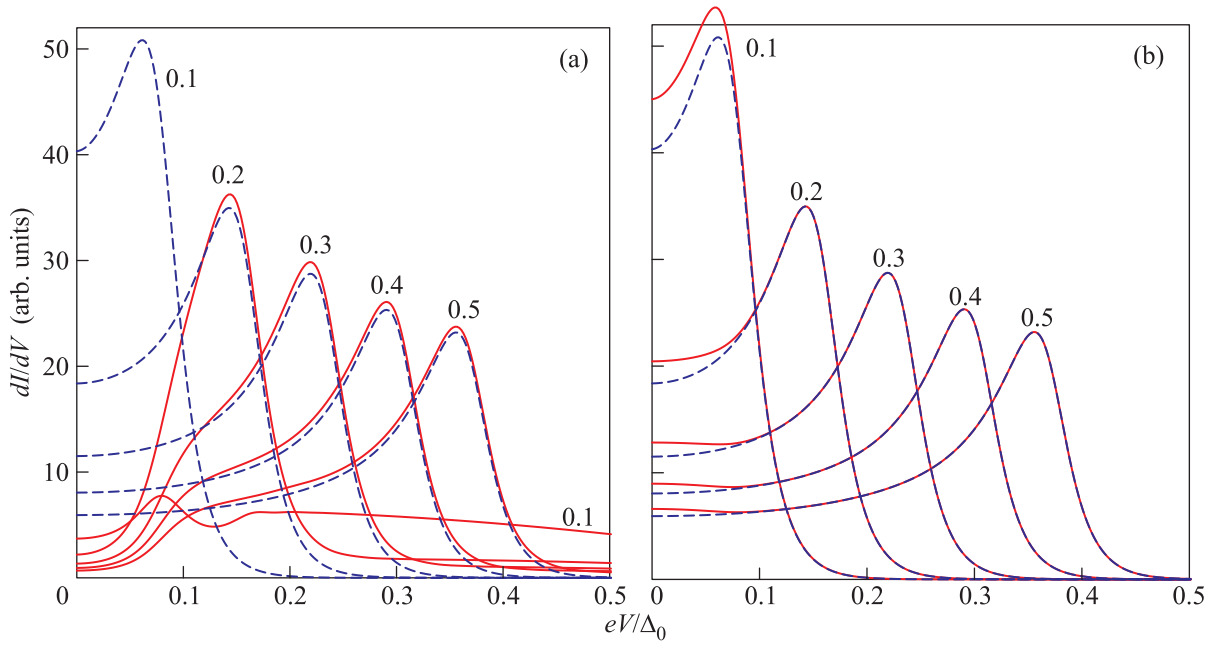

Fig. 6. (Color online) The local differential conductance vs the voltage V for both vortex types. Blue dashed lines correspond to a free vortex dI/dV pattern. Here we put $R = 0.1\xi$, $T = 0.02\Delta_0$

based on the full Bogolubov–e Gennes equations appear to be in a good agreement with the quasiclassical results presented above (though the inversion of the spectral branch slope for N_+ vortices has been overlooked in the previous work [33]).

The peculiarities of the quasiparticle spectrum reveal certainly in the LDOS pattern. Substituting the spectrum in the formula (20) one can obtain the local conductance profile shown in Fig. 6 both for N_+ and N_- vortices. The conductance for the N_- vortex (Fig. 6b) reveals the typical CdGM behavior for $r > R$. This conclusion is no more valid if we consider N_+ vortex where the large slope of the inversed anomalous branch causes strong changes in the LDOS pattern (Fig. 6a). The local conductance distribution in this case is similar to the one for a pinned vortex in the s-wave superconductor considered above [11].

The above strong difference in the subgap spectra for N_+ and N_- vortices should of course reveal in the difference in the pinning potentials for the opposite magnetic field orientations. The additional spectral branches which appear around the defect in the presence of the N_+ vortex are gapped similarly to the ones in the s-wave superconductors. Thus, one can expect that the depinning current density should be given by a similar estimate based on the Landau-type criterion. The absence of the gap in the spectral branch of the N_- vortex indicates definitely a weaker pinning energy which in this case should originate from the delocalized excitations above the gap Δ_0. This dependence of the individual pinning force on the magnetic field orientation is specific for p-wave superconductors and can be detected by standard measurements of the depinning current density vs magnetic field orientation.

4. Microwave response of pinned vortices. Besides the STM/STS studies there exists another powerful method for experimental investigation of quasiparticle subgap spectrum based on the measurements of the conductivity tensor at finite frequencies. Considering the subgap excitations corresponding to a certain spectral branch $\varepsilon(b)$ crossing the Fermi level one can describe the interaction of the quasiparticles with the high-frequency field using the Hamiltonian (22). In London limit the superfluid velocity $\mathbf{V}$ is proportional to the vector potential $\mathbf{V} = -e/(mc)\mathbf{A}$. Taking a circularly polarized field $\mathbf{V}$ with the frequency Ω we obtain the following Hamiltonian:

$$H(\mu,\theta) = \varepsilon(\mu) - \frac{2e\hbar k_{\mathrm{F}}}{mc}\mathrm{Re}\left(A_{\pm}e^{\pm i\theta - i\Omega t}\right), \qquad (33)$$

where the sign "+"or "−"denotes the circular polarization orientation and $A_{\pm}$ is the complex amplitude, i.e., the total magnetic potential is $\mathbf{A} = \mathrm{Re}\left[e^{-i\Omega t}A_{\pm}(\mathbf{x}_0 \pm i\mathbf{y}_0)\right]$. In order to find the conductivity tensor one should follow then the procedure described, e.g., in [8] solving the Boltzmann equation written for the quasiparticle distribution function. The

resulting expressions for the Ohmic and Hall conductivities read:

$$\sigma_{\rm O} = \frac{e^2 k_{\rm F}}{2m\Omega} \frac{\nu + i\Omega}{(\nu + i\Omega)^2 + \omega_0^2}, \tag{34}$$

$$\sigma_{\rm H} = -\frac{e^2 k_{\rm F}}{2m\Omega} \frac{\omega_0}{(\nu + i\Omega)^2 + \omega_0^2}, \tag{35}$$

where $\hbar\omega_0 = \partial\varepsilon/\partial\mu|_{\varepsilon=0}$ and ν is the quasiparticle relaxation rate. One can see that the sign and the value of the Hall conductivity are strongly determined by the slope of the anomalous spectral branch at the Fermi level. The Hall conductivity can be probed experimentally, e.g., by the polar Kerr effect measurements [30].

The spectral branches which do not cross the Fermi level are not described by the above expressions and can not contribute to the dissipation at low frequencies Ω since the quasiparticle spectral flow from $-\Delta_0$ to $+\Delta_0$ is suppressed due to the presence of the minigap $\Delta_m(R) \sim \Delta_0 R/\xi$ dependent on the defect radius. Thus, one can clearly distinguish two regimes in the behavior of the microwave response of pinned vortices depending on the ratio of the microwave frequency to the value Δ_m. In the low frequency regime $\Omega \ll \Delta_m$ the dissipation accompanying pinned vortex oscillations in s-wave superconductors should be suppressed and the dominant response should correspond to the Hall part of the conductivity tensor. The increase of frequency above the threshold Δ_m should cause a strong increase in the dissipation rate [13]. In p-wave superconductors such behavior with the threshold in the microwave frequency can be observable only for N_+ vortices, i.e., only for one orientation of the magnetic field. The microwave conductivity tensor for the opposite magnetic field orientation (N_- vortices) should differ only slightly from the one describing the motion of free vortices. An obvious difference of the dynamics of the N_+ vortices from the s-wave case should be caused certainly by the appearance of an additional spectral branch with the slope coinciding with the one for the quasiparticle edge states in the vortex free configuration. The contribution of this branch to the conductivity tensor does not differ from the one provided by the defects themselves. To sum up we get a strong asymmetry of both the dissipative and Hall responses at microwave frequencies as we change the magnetic field direction which is peculiar for p-wave superconductivity. This asymmetry can be used as an experimental test for the chiral superconducting order parameter.

The above analysis shows that the magnetotransport measurements on the samples with columnar defects can be considered as a useful tool for probing the quasiparticle spectra and gap symmetry in the superconducting compounds. The experimental data on the magnetic field dependence of the dc depinning current density and the frequency dependence of the microwave response can give us a valuable information about the electronic structure of pinned vortices and help to distinguish the materials with conventional and chiral superconducting orders. The deeper understanding of the electronic structure of the pinned vortex states can also be useful for the control of the vortex pinning in the artificial superconducting structures with antidots providing a simple criterion of the stability of multiquanta vortex configurations.

This work was supported by the Dynasty Foundation (VLV), Russian Foundation for Basic Research (ASM), and Russian Science Foundation under Grant # 15-12-10020 (AVS).

1. G. S. Mkrtchyan and V. V. Shmidt, Sov. Phys. JETP **34**, 195 (1972).
2. A. Buzdin and D. Feinberg, Physica C **256**, 303 (1996).
3. A. Buzdin and M. Daumens, Physica C **294**, 257 (1998).
4. H. Nordborg and V. M. Vinokur, Phys. Rev. B **62**, 12408 (2000).
5. E. V. Thuneberg, J. Kurkijarvi, and D. Rainer, Phys. Rev. Lett. **48**, 1853 (1982).
6. E. V. Thuneberg, J. Kurkijarvi, and D. Rainer, Phys. Rev. B **29**, 3913 (1984).
7. E. V. Thuneberg, J. Low Temp. Phys. **57**, 415 (1984).
8. N. B. Kopnin, *Theory of Nonequilibrium Superconductivity*, Oxford University, N.Y. (2001).
9. C. Caroli, P. G. de Gennes, and J. Matricon, Phys. Lett. **9**, 307 (1964).
10. C. W. J. Beenakker, Phys. Rev. Lett. **67**, 3836 (1991).
11. A. S. Mel'nikov, A. V. Samokhvalov, and M. N. Zubarev, Phys. Rev. B **79**, 134529 (2009).
12. G. E. Volovik, PisTma v ZhETF **57**, 233 (1993) [JETP Lett. **57**, 244 (1993)].
13. B. Rosenstein, I. Shapiro, E. Deutch, and B. Ya. Shapiro, Phys. Rev. B **84**, 134521 (2011).
14. A. S. Mel'nikov and A. V. Samokhvalov, Pis'ma v ZhETF **94**, 823 (2011).
15. M. Baert, V. V. Metlushko, R. Jonckheere, V. V. Moshchalkov, and Y. Bruynseraede, Phys. Rev. Lett. **74**, 3269 (1995).
16. A. V. Silhanek, S. Raedts, M. J. Van Bael, and V. V. Moshchalkov, Phys. Rev. B **70**, 054515 (2004).
17. A. I. Buzdin, Phys. Rev. B **47**, 11416 (1993).
18. A. Bezryadin, A. Buzdin, and B. Pannetier, Phys. Lett. A **195**, 373 (1994).
19. G. Karapetrov, J. Fedor, M. Iavarone, D. Rosenmann, and W. K. Kwok, Phys. Rev. Lett. **95**, 167002 (2005).

20. I. V. Grigorieva, W. Escoffier, V. R. Misko, B. J. Baelus, F. M. Peeters, L. Y. Vinnikov, and S. V. Dubonos Phys. Rev. Lett. **99**, 147003 (2007).
21. Y. Tanaka, S. Kashiwaya, and H. Takayanagi, Jpn. J. Appl. Phys. **34**, 4566 (1995).
22. M. Eschrig, D. Rainer, and J. A. Sauls, in *Vortices in Unconventional Superconductors and Superfluids* (2001), p. 175.
23. A. S. Mel'nikov and V. M. Vinokur, Nature **415**, 60 (2002).
24. A. S. Mel'nikov and M. A. Silaev, Pis'ma v ZhETF **83**, 675 (2006) [JETP Lett. **83**, 578 (2006)].
25. A. S. Mel'nikov, D. A. Ryzhov, and M. A. Silaev, Phys. Rev. B **78**, 064513 (2008).
26. M. M. Virtanen and M. M. Salomaa, Phys. Rev. B **60**, 14581 (1999).
27. N. Schopohl and K. Maki, Phys. Rev. B **52**, 490 (1995); N. Schopohl, arXiv:9804064 (unpublished).
28. L. Kramer and W. Pesch, Z. Phys. **269**, 59 (1974).
29. V. L. Vadimov and A. S. Mel'nikov, arXiv:1412.6992 [cond-mat.supr-con].
30. C. Kallin, Rep. Prog. Phys. **75**, 042501 (2012).
31. Yu. S. Barash and A. S. Mel'nikov, ZhETF **100**, 307 (1991) [Sov. Phys. JETP **73**, 170 (1991)].
32. B. Y. Shapiro et al., to be published.
33. B. Rosenstein, I. Shapiro, and B. Y. Shapiro, J. Phys.: Cond. Mat. **25**, 075701 (2013).